Materials Science Forum
ISSN: 1662-9752, Vol. 1192, pp 89-96
doi:10.4028/p-U2bkIl

Submitted: 2025-09-23
Revised: 2026-01-07
Accepted: 2026-01-31
Online: 2026-05-20

Influence of Different Contact Lengths on the Correct Extraction of the Resistance Parameters of TLM Test Structures on 4H-SiC

Maximilian Ley[1,a*], Julian Kauth[1,b], Mathias Rommel[1,c], Björn Fischer[2,d], Alexander May[1,e], and Jörg Schulze[1,3,f]

[1]Fraunhofer Institute for Integrated Systems and Device Technology (IISB), Schottkystraße 10, 91058 Erlangen, Germany

[2]Infineon Technologies AG, Am Campeon 1-15, 85579 Neubiberg, Germany

[3]Chair of Electron Devices, Friedrich-Alexander-Universität Erlangen-Nürnberg, Cauerstraße 6, 91058 Erlangen, Germany

[a]maximilian.ley@iisb.fraunhofer.de, [b]julian.kauth@iisb.fraunhofer.de, [c]mathias.rommel@iisb.fraunhofer.de, [d]bjoern.fischer@infineon.com, [e]alexander.may@iisb.fraunhofer.de, [f]joerg.schulze@fau.de

Keywords: TLM Test Structure, Contact Length, TCAD, 4H-SiC, Contact end Resistance, Sheet Resistance, Specific Contact Resistivity, Transfer Length, Simulation Analysis, Ohmic Contact

Abstract. Accurate characterization of low-resistance ohmic contacts on 4H-SiC is crucial for device development, but is complicated by the limitations of the standard Transfer Length Method (TLM). TLM test structures are widely used for extracting the specific contact resistivity (ρ_{C}) between metal and semiconductor layers, as well as the sheet resistance of doped layers. The contact formation process itself, particularly the annealing step, modifies the SiC layer under the contact. This results in a sheet resistance below the contact (R_{SK}) that deviates from the sheet resistance of interest between the contacts (R_{SH}), which invalidates a key assumption of the standard TLM evaluation of a constant R_{SH} throughout the whole TLM test structure. This study uses 2D TCAD simulation of TLM test structures to investigate the influence of the contact length L, while using an advanced evaluation method for extracting ρ_{C} with the help of a third contact. Consequently, it is necessary to measure the contact end resistance R_{CE}, which is derived from the potential at the end of the TLM contact. The findings provide a deeper understanding of the TLM technique's robustness and offer valuable guidelines for optimizing TLM test structures to ensure accurate characterization of ohmic contacts on 4H-SiC.

Introduction

In recent years, 4H-Silicon Carbide (4H-SiC) has emerged as a leading semiconductor material for high-power, high-frequency, and high-temperature electronic devices, owing to its superior material properties, including a wide bandgap, high critical electric field, and excellent thermal conductivity [1]. The overall performance and energy efficiency of these devices are critically dependent on the quality of the metal-semiconductor interface, specifically the formation of low-resistance ohmic contacts. However, achieving such contacts on 4H-SiC is challenging compared to silicon, primarily due to three factors: Its wide bandgap creates a large Schottky barrier, its chemical inertness complicates surface preparation, and there is a lack of metals with suitable work functions [2]. To characterize and optimize ohmic contacts, the Transfer Length Method (TLM) has become an industry-standard technique [2]. The standard TLM evaluation allows for the extraction of the specific contact resistivity (ρ_{C}) and the sheet resistance (R_{SH}) of the semiconductor layer between the contacts [3]. The accuracy of these extracted parameters is highly dependent on the design of the TLM test structure and the assumptions made during the analysis [4, 2].
This work presents a systematic simulation-based study using TCAD Sentaurus [5] to investigate and quantify the impact of the contact length L on the extraction of contact front resistance R_{CF} and contact end resistance R_{CE} in 4H-SiC TLM test structures. Scenarios where R_{SK} and R_{SH} differ are analyzed, exploring the conditions where the regular TLM analysis comes to its limits.

Standard TLM Evaluation and Parameter Extraction

According to the standard TLM evaluation, the total resistance R_T measured between two adjacent ohmic contacts is linearly dependent on the spacing d_i between them, as described by the following equation [4]:

$$R_T = (R_{SH}/Z)d + 2R_{CF} \tag{1}$$

Here, R_{CF} is the contact resistance, R_{SH} is the sheet resistance of the doped semiconductor layer, and Z is the contact width of the TLM test structure. The standard model relies on the assumption of a uniform sheet resistance ($R_{SH} = R_{SK}$) [6, 7]. In this work, ideal material properties and interfaces are assumed in the simulation, resulting in a linear relationship between R_T and d_i (i.e., with a coefficient of determination $R^2 = 1$), this criterion is not always matched in real measurements. The analytical procedure begins by determining R_T from simulated current-voltage (I-V) characteristics for a range of different contact spacings d_i. The resistance values are then plotted as a function of d, as shown in Fig. 1. A linear regression applied to this data allows for the extraction of key parameters: The slope of the fit yields R_{SH}/Z, the y-axis intercept corresponds to $2R_{CF}$, and the x-axis intercept corresponds to $-2L_T$. L_T is the distance after which the potential under the contact drops to $1/e$, i.e., it describes

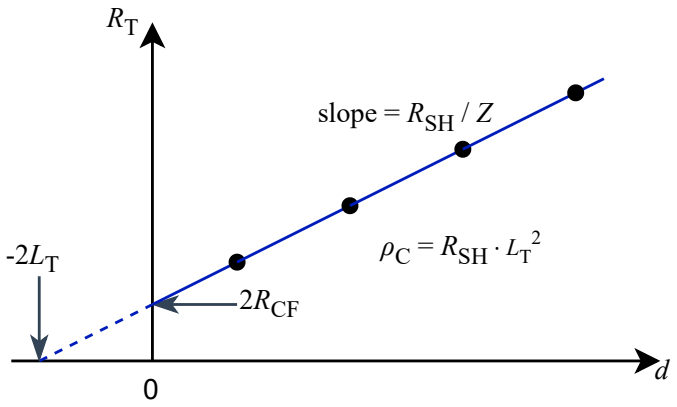

Fig. 1: Graphical representation of the standard TLM evaluation. The total resistance R_T is plotted against the contact spacing d. The sheet resistance R_{SH} is extracted from the slope of the linear fit, while the contact resistance R_{CF} and transfer length L_T are determined from the y- and x-axis intercepts, respectively.

the length of the contact that mainly contributes to the current flow and is calculated by the following equation:

$$L_T = R_{CF} \cdot Z/R_{SH} \tag{2}$$

The specific contact resistivity ρ_C, which is a measure of the contact quality independent on geometry, can be calculated either through the $coth$, which considers the potential distribution under the contact, or by an approximation, which is only valid for long contacts ($L \gg L_T$) [4]:

$$\rho_C = R_{CF} \cdot L_T \cdot Z/\coth(L/L_T) \qquad \rho_C = R_{SH} \cdot L_T^2 \tag{3}$$

TLM Evaluation with Contact End Resistance

To account for the discrepancy between R_{SK} and R_{SH}, the evaluation can be extended by additionally measuring the contact end resistance R_{CE} [8]. R_{CE} describes the resistance at the trailing edge of the

TLM contact. The contact front resistance R_{CF} and the contact end resistance R_{CE} can be derived as [4]:

$$R_{\mathrm{CF}} = \frac{V(x=0)}{I(x=0)} = \frac{\sqrt{R_{\mathrm{SK}}\rho_{\mathrm{C}}}}{Z}\coth\left(L/L_{\mathrm{Tk}}\right) = \frac{\rho_{\mathrm{C}}}{L_{\mathrm{Tk}}Z}\coth\left(L/L_{\mathrm{Tk}}\right) \tag{4}$$

$$R_{\mathrm{CE}} = \frac{V(x=L)}{I(x=0)} = \frac{V_{\mathrm{CE}}}{I} = \frac{\sqrt{R_{\mathrm{SK}}\rho_{\mathrm{C}}}}{Z}\frac{1}{\sinh\left(L/L_{\mathrm{Tk}}\right)} = \frac{\rho_{\mathrm{C}}}{L_{\mathrm{Tk}}Z}\frac{1}{\sinh\left(L/L_{\mathrm{Tk}}\right)} \tag{5}$$

Here, L is the contact length, and L_{Tk} is the transfer length defined as $L_{\mathrm{Tk}} = \sqrt{\frac{\rho_c}{R_{\mathrm{SK}}}}$. Note that L_{Tk} is the true transfer length under the contact, which may differ from the apparent transfer length L_{T} extracted from the standard TLM plot, as L_{T} is derived assuming $R_{\mathrm{SK}} = R_{\mathrm{SH}}$. The ratio of R_{CE} to R_{CF} depends only on L relative to L_{Tk}:

$$\frac{R_{\mathrm{CE}}}{R_{\mathrm{CF}}} = \frac{1}{\cosh\left(L/L_{\mathrm{Tk}}\right)} \tag{6}$$

This relationship, in combination with Eq. 4 and 5, allows the determination of L_{Tk}, ρ_{C}, and R_{SK}. L_{Tk} can be calculated by rearranging the resistance ratio equation:

$$L_{\mathrm{Tk}} = \frac{L}{\operatorname{arcosh}\left(R_{\mathrm{CF}}/R_{\mathrm{CE}}\right)} \tag{7}$$

With L_{Tk} known, ρ_{C} is calculated without the implicit assumption of $R_{\mathrm{SK}} = R_{\mathrm{SH}}$, which does not account for a differing R_{SK}:

$$\rho_{\mathrm{c}} = \frac{L_{\mathrm{Tk}} \cdot Z \cdot R_{\mathrm{CE}}}{\sinh\left(L/L_{\mathrm{Tk}}\right)} \tag{8}$$

Finally, R_{SK} is determined using the definition of L_{Tk}:

$$R_{\mathrm{SK}} = \frac{\rho_{\mathrm{C}}}{L_{\mathrm{Tk}}^2} \tag{9}$$

The advanced analysis with R_{CE} enables a more accurate determination of ρ_{C} and an insight into the impact of the contact fabrication on the underlying semiconductor layer.

Simulation Methodology

A three-contact TLM test structure is investigated in 2D using Synopsys TCAD Sentaurus, using standard physics models for 4H-SiC, including models for doping-dependent mobility and incomplete ionization of dopants. The simulated structure, depicted in Fig. 2, consists of a p-type doped layer on a lightly doped n-type epitaxial layer with a background concentration of $1 \times 10^{15}\,\mathrm{cm}^{-3}$. The doping of the p-type implanted layer is fixed to a concentration of $1 \times 10^{19}\,\mathrm{cm}^{-3}$. The specific contact resistivity is set to $\rho_{\mathrm{C}} = 0.5\,\mathrm{m\Omega\,cm}^2$. To investigate the impact of the contact processing, the sheet resistance directly under the contacts R_{SK} was independently controlled by varying the net active doping concentration within the top $100\,\mathrm{nm}$ of this implanted layer. This setup allows for a systematic study of the effects of a non-uniform sheet resistance ($R_{\mathrm{SK}} \neq R_{\mathrm{SH}}$). R_{CE} is determined by measuring the potential at contact C3. This potential is identical to the potential of the trailing edge ($x = L$) of the current-carrying contact C2 relative to the leading edge ($x = 0$) of C2, where the current injection takes place. Contact C3 is modeled as a floating voltage probe by constraining its current to zero. The resistance value of R_{CE} is independent on the spacing d_{i} between the contacts, but strongly dependent on L and the sheet resistance of the layers under the contact. Current-Voltage (I-V) characteristics (Fig. 3) are simulated across a range of contact lengths L and contact spacings d_{i} by sweeping the voltage and measuring the current between the contacts C1 and C2. This approach addresses a significant limitation of the standard TLM evaluation: The assumption of a uniform sheet resistance ($R_{\mathrm{SH}} = R_{\mathrm{SK}}$), which is often invalid in practice. For instance, forming nickel silicide ($\mathrm{Ni}_x\mathrm{Si}_y$) contacts to n-type SiC

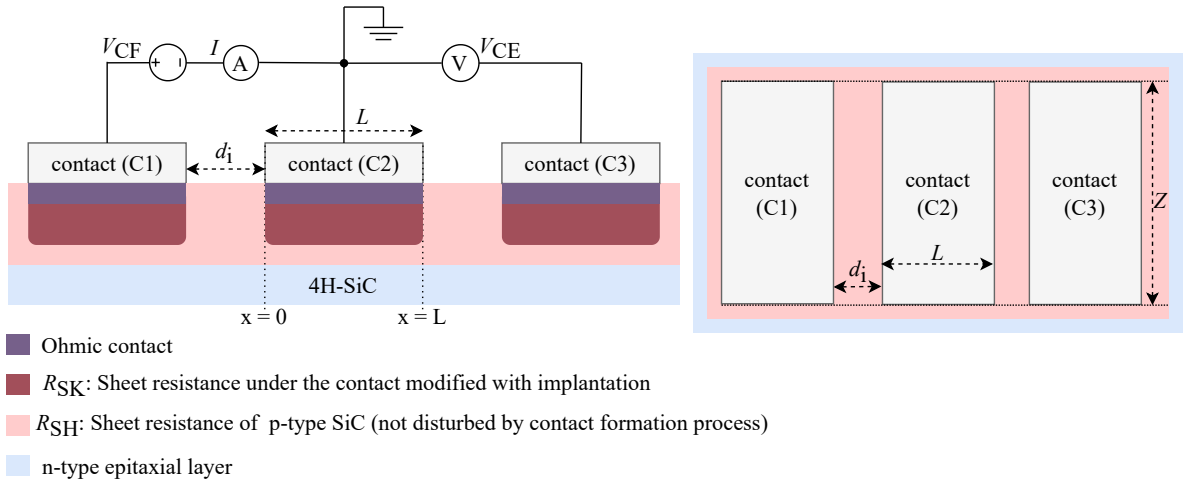

Fig. 2: Cross-section and top view schematic of the simulated device for a TLM test structure with a third contact, which serves as a voltage probe.

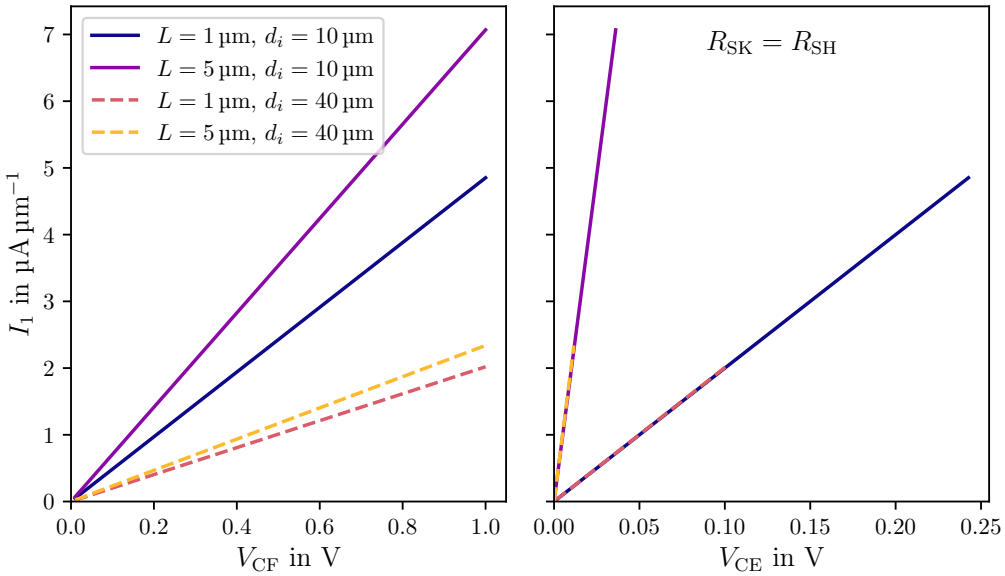

Fig. 3: I-V characteristic for two different d_i and L for determining the resistance values for the standard TLM evaluation (left) and R_{CE} (right).

selectively consumes silicon [9], while forming TiAl-based contacts to p-type SiC consumes SiC to form Ti_xSiC_y [10]. Both processes alter the stoichiometry and doping profile, leading to a discrepancy ($R_{SK} \neq R_{SH}$) that can cause errors in the extracted ρ_C.

The measurement of R_{CE} enables the separation of the sheet resistances R_{SK} from R_{SH}, leading to a more accurate determination of ρ_C [11]. However, the ability to accurately measure R_{CE} depends on the geometric design. The contact length L must be carefully chosen relative to the contact length [3] as shown in the simulation data presented in the following sections. The simulation results are normalized to a standard device width of $Z = 1\,\mu m$, which corresponds to the contact width. R_{SK} is controlled independently of R_{SH} by defining a separate net doping concentration in that region. This idealized approach allows for a direct investigation of the impact of the R_{SK}/R_{SH} ratio on the extracted parameters, decoupled from the complex and process-specific physics of contact formation.

The simulation procedure is designed to extract R_{CF} and R_{CE}. To determine R_{CF}, the total resistance R_T between adjacent contacts is simulated for several structures with systematically varied contact

spacings d_i. R_CF is then extracted from the y-intercept of a linear fit of R_T versus d and R_SH from the slope of the same plot, consistent with the standard TLM analysis:

$$R_T = V_\mathrm{CF}(d)/I(d) \tag{10}$$

To determine R_CE, the current I between C1 and C2 is measured, and the potential difference between the current-carrying contact C2 and the floating contact C3 is recorded. R_CE is then calculated by:

$$R_\mathrm{CE} = V_\mathrm{CE}/I \tag{11}$$

The entire procedure is repeated for different L and $R_\mathrm{SK}/R_\mathrm{SH}$ to analyze their combined influence on the extracted parameters.

Discussion of Simulation Results

Fig. 4 compares the ideal case ($R_\mathrm{SK} = R_\mathrm{SH}$) with a uniform sheet resistance across the TLM test structure with a more realistic scenario where the sheet resistance under the contact is higher ($R_\mathrm{SK} > R_\mathrm{SH}$). The specific contact resistivity ρ_C and sheet resistance values extracted from these linear fits show

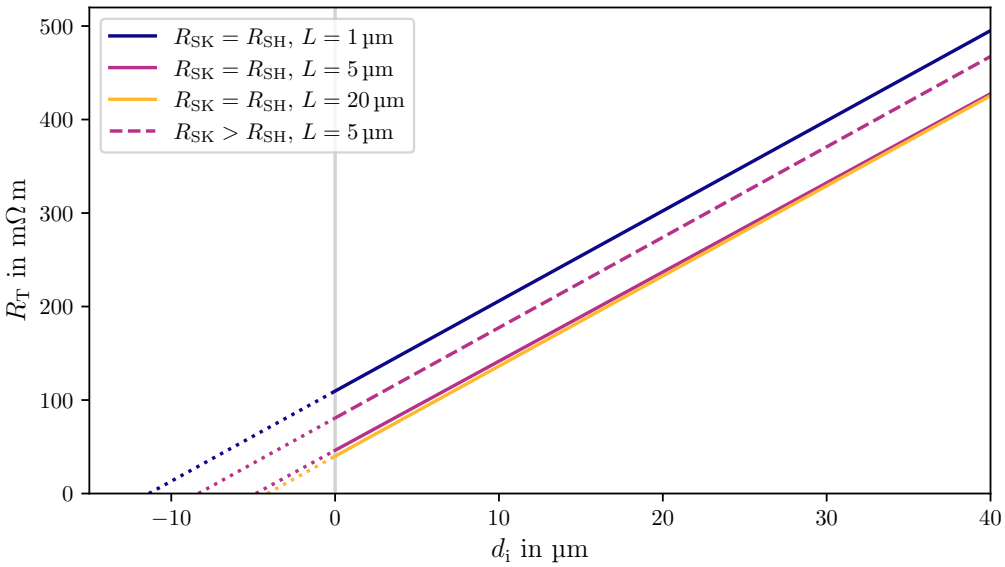

Fig. 4: Standard TLM evaluation plot: R is shown in dependence on d_i for different contact lengths L, for $L = 5\,\mu\mathrm{m}$ also the case of $R_\mathrm{SK} > R_\mathrm{SH}$ is shown.

good agreement with the input parameters of the simulation for the ideal case, confirming the validity of the model and the extraction methodology.
When $R_\mathrm{SK} > R_\mathrm{SH}$, the total measured resistance increases, resulting in a significantly larger y-intercept. A standard TLM analysis would erroneously attribute this entire increase to a higher R_CF, leading to an inaccurate calculation of the specific contact resistivity ρ_C. These simulations underscore the necessity of measuring R_CE to correctly separate the different resistance contributions. As seen in Fig. 4, using a contact length L shorter than L_T results in a higher extracted R_CF. Meanwhile, increasing L reduces the contact resistance only up to a certain limit, with similar y-axis intercepts observed for $L = 5\,\mu\mathrm{m}$ and $L = 20\,\mu\mathrm{m}$ in Fig. 4).

Impact of contact length L on extracted resistances. L has a significant effect on the extracted values of R_CE. This relationship is illustrated in Fig. 5, which shows the simulated resistances as a function of L. The data reveals a design trade-off for accurate parameter extraction. While R_CF remains largely independent of the contact length for $L > L_\mathrm{T}$, R_CE shows a strong dependence.

For short contacts ($L \approx L_T$), R_{CE} is easily measurable, but becomes sensitive to manufacturing variations in L. In contrast, for long contacts ($L \gg L_T$), R_{CE} diminishes exponentially and approaches zero. Thus, a correct extraction of R_{CE} is not possible due to measurement limitations. The observed trend

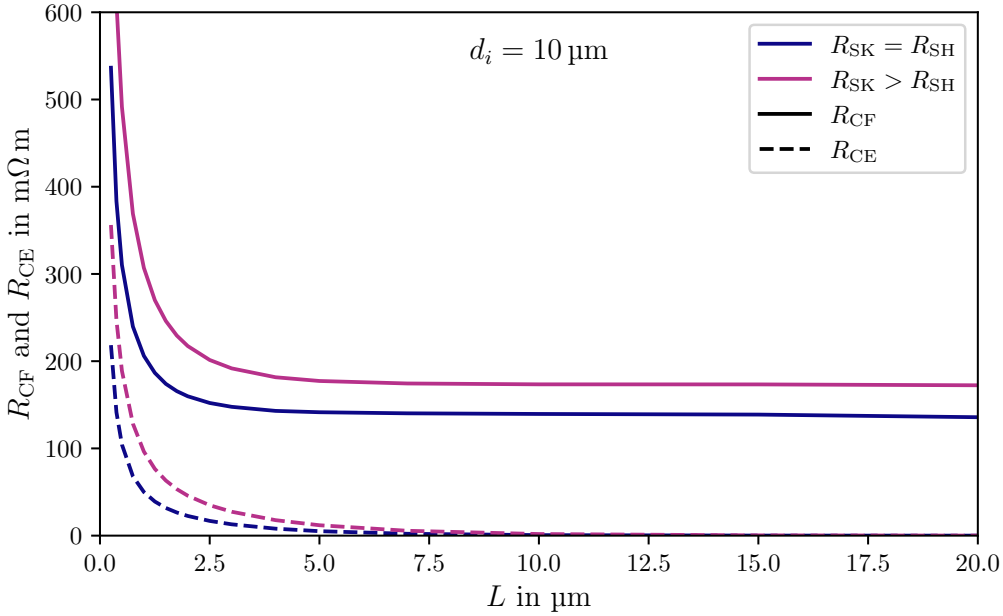

Fig. 5: Dependence of R_{CF} and R_{CE} on the contact length L shown for different R_{SH} and R_{SK}. R_{CE} is approaching zero and thus not measurable for large L. Meanwhile, R_{CF} shows an asymptotic approach to a fixed value for large L. The distance between contact C2 and C3 is equal to the one between C1 and C2 in this simulation, the value of R_{CE} is independent of the spacing d_i.

in Fig. 5 reveals a fundamental trade-off. For $L \gg L_T$ the current transfer is essentially completed well before the physical end of the contact. Consequently, V_{CE} (and thus R_{CE}) becomes vanishingly small. In an experimental setting, this small voltage would be lost in the measurement noise, making an accurate extraction of R_{CE} impossible. Without a reliable R_{CE} value, the separation of R_{SK} from R_{SH} is not possible. For short contacts, small absolute variations represent large percentual variation in L, making the extracted values of R_{CE} highly susceptible to manufacturing tolerances, leading to poor statistical reproducibility across a wafer. Consequently, an effective design requires a L comparable to the contact's specific L_T. This is a critical consideration for 4H-SiC, where L_T can vary significantly (e.g., $L_T \approx 0.5\,\mu m$ for contacts to n-type SiC vs. $L_T \approx 4\,\mu m$ for contacts to p-type SiC - this data was extracted by using the standard TLM evaluation) [12].

Comparison between ρ_C values from both analyses. To quantify the error introduced by the standard TLM evaluation, we compared ρ_C obtained from the two different sets of equations explained in the previous section: For the standard analysis, ρ_C is calculated using the standard TLM evaluation with and without the approximation for the $coth$ according to Eq. 3, which assumes a uniform sheet resistance ($R_{SK} = R_{SH}$). In contrast, for the TLM analysis with R_{CE}, ρ_C is calculated using the more comprehensive model that incorporates the measured R_{CE}, as described in Eq. 8.

The results are plotted in Fig. 6. For the more realistic scenario with $R_{SK} > R_{SH}$, the standard analysis significantly overestimates the true ρ_C (grey dotted line). In contrast, the TLM analysis with R_{CE}, which accounts for the non-uniformity, extracts ρ_C more accurately. This result confirms that the R_{CE} measurement is essential for the accurate characterization of real ohmic contacts. For the case of $R_{SK} = R_{SH}$, both methods yield similar results as expected.

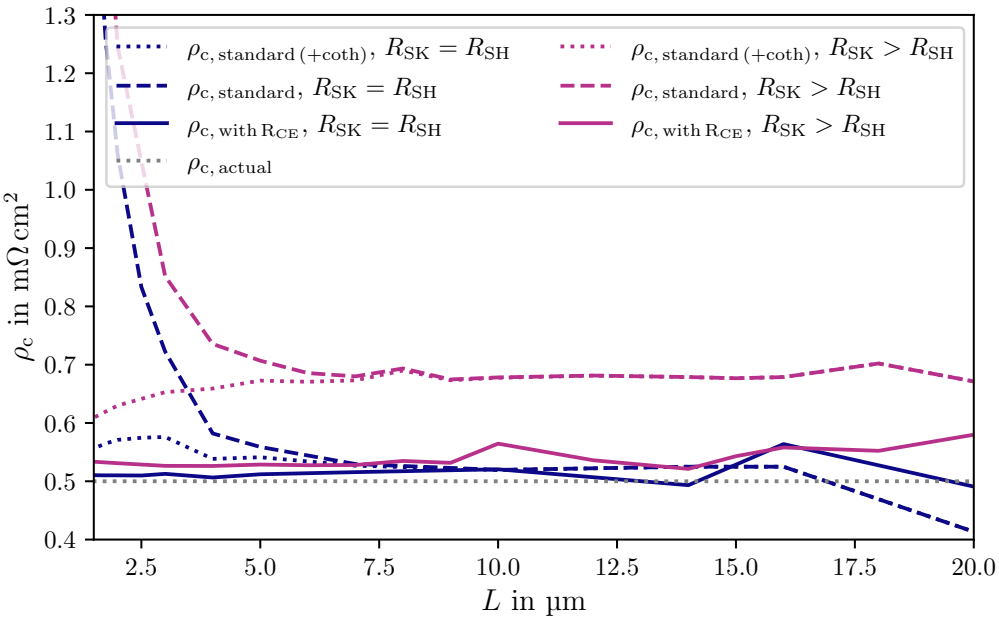

Fig. 6: ρ_C determination with different evaluation routines are shown. The ρ_C determination with R_{CE} is more accurate for $R_{SK} > R_{SH}$, while there is no significant difference for the ideal case of $R_{SK} = R_{SH}$.

Conclusion

Through 2D TCAD simulations, this work has quantitatively demonstrated that the contact length L is a critical design parameter for the accurate characterization of 4H-SiC ohmic contacts using R_{CE}, i.e., the determination of ρ_C and the decoupling of R_{SK} and R_{SH}. This implies that TLM test structures must be carefully designed: L must be within the range of the transfer length. This makes L a critical design parameter, as L_T is not a fixed value. Contacts to n- and p-type 4H-SiC require different L, as their respective processing conditions and contact schemes yield significantly different transfer lengths L_T. L_T strongly depends on the contact material and the semiconductor doping. Therefore, an optimized TLM design for different contacts and materials is required. Measuring R_{CE} is essential for correctly determining the specific contact resistivity (ρ_C) in realistic scenarios where the sheet resistance is non-uniform ($R_{SK} \neq R_{SH}$). Adopting these guidelines will enable the design of more accurate TLM test structures.

References

[1] T. Kimoto, *Fundamentals of silicon carbide technology*. John Wiley & Sons Singapore Pte. Ltd, 2014.

[2] K. Zekentes and K. Vasilevskiy, *Advancing Silicon Carbide Electronics Technology I*, vol. 37. Materials Research Forum LLC, 2018.

[3] G. K. Reeves and H. B. Harrison, "Obtaining the specific contact resistance from transmission line model measurements," vol. 3, no. 5, pp. 111–113, 1982.

[4] D. K. Schroder, *Semiconductor material and device characterization*. IEEE Press and Wiley, 3rd ed. ed., 2006.

[5] Synopsys, "Sentaurus™ device user guide."

[6] S. Oussalah, B. Djezzar, and R. Jerisian, “A comparative study of different contact resistance test structures dedicated to the power process technology,” vol. 49, no. 10, pp. 1617–1622, 2005.

[7] H.-J. Ueng, D. B. Janes, and K. J. Webb, “Error analysis leading to design criteria for transmission line model characterization of ohmic contacts,” vol. 48, no. 4, pp. 758–766, 2001.

[8] G. K. Reeves and B. Harrison, “An analytical model for alloyed ohmic contacts using a trilayer transmission line model,” vol. 42, no. 8, pp. 1536–1547, 1995.

[9] S. Y. Han, K. H. Kim, J. K. Kim, H. W. Jang, K. H. Lee, N.-K. Kim, E. D. Kim, and J.-L. Lee, “Ohmic contact formation mechanism of ni on n-type 4h–sic,” vol. 79, no. 12, pp. 1816–1818, 2001.

[10] S. Tsukimoto, K. Ito, Z. Wang, M. Saito, Y. Ikuhara, and M. Murakami, “Growth and microstructure of epitaxial ti_3sic_2 contact layers on sic,” vol. 50, no. 5, pp. 1071–1075, 2009.

[11] W. M. Loh, S. E. Swirhun, T. A. Schreyer, R. M. Swanson, and K. C. Saraswat, “Modeling and measurement of contact resistances,” vol. 34, no. 3, pp. 512–524, 1987.

[12] M. Rommel, A. May, L. Baier, J. Kauth, N. Bottcher, and M. Jank, “Investigation of ohmic contacts and resistances of a 4h-sic cmos technology up to 550 degrees c,” vol. 21, no. 4, 2024.